Combinatorial Methods for Polymer Materials Science:
Phase Behavior of Nanocomposite Blend Films

ALAMGIR KARIM[1*], KORAY YUREKLI[2], CARSON MEREDITH[3],
ERIC AMIS[1], *and* RAMANAN KRISHNAMOORTI[2]

[1]*Polymers Division, NIST*
Gaithersburg, MD 20899

[2]*Department of Chemical Engineering, University of Houston*
4800 Calhoun, Houston, TX 77204-4004

[3]*School of Chemical Engineering*
Georgia Institute of Technology, 778 Atlantic Dr.
Atlanta, GA 30332-0100

Polymer materials are often mixed with inorganic materials in the bulk to enhance properties, including mechanical, electrical, thermal, and physical. Such property enhancements are induced not only by the physical presence of the filler but also significantly by the interaction of the polymer with the filler via altering the local properties of the polymer material. In this regard, recently layered silicate nanocomposites have been shown to be effective in modifying the polymer properties because of their high surface area of contact between the polymer and the high aspect ratio nanoparticle. Potential property enhancements should also occur in polymer nanocomposite thin films owing to nanoparticle orientation from film confinement effects. In this paper we investigate the effect of layered silicate nanoparticles on the phase behavior of a classic polymer blend using small angle neutron scattering and compare those results to phase diagrams obtained by high throughput combinatorial methods.

INTRODUCTION

Recently, much interest has focused on the enhanced thermal, mechanical, barrier, and ablation properties of layered-silicate based polymer nanocomposites (1–7). Considerable interest has focused on the potential enhancement in barrier properties of these nanocomposites, as it directly relates to one of their most important potential applications in both traditional and cutting edge technologies (5–8). In particular, the thin film phase behavior of polymer-based layered-silicate nanocomposites has proven to be extremely interesting because of the ability to alter the phase behavior of the polymer using small amounts of added layered silicate (9–11). In this context, we report here the influence of addition of highly anisotropic layered silicates in altering the phase behavior of binary blends of polystyrene and polyvinylmethylether (PS/ PVME) (12) both in the bulk and in thin films. Previous studies have examined the thermodynamics of mixing of homopolymers with layered silicates (13) and the influence of layered silicates on block copolymer ordering (14–16) and have demonstrated the significant potential for nucleation of ordered structure in such materials.

On another front, owing to successes in pharmaceuticals research, combinatorial and high-throughput methods for searching composition space have received increasing attention for the synthesis and discovery of new inorganic materials, catalysts, and organic polymers (17). Combinatorial methods can also allow rapid scanning of parameter space to make fundamental measurements and develop physical models for polymers (18, 19). One limitation is the difficulty of preparing parallel libraries and performing high-throughput screening with conventional instrumentation and sample preparation techniques.

We present combinatorial methods for measuring important fundamental properties of polymer thin films: phase behavior of polymer blends and the effect of layered-silicate additive on the phase separated

---

*Corresponding author.

morphology. Library creation, high-throughput measurements, and informatics are used to generate combinatorial maps of wettability and phase behavior. The temperature and composition dependence of the phase boundary for a PS/PVME blend film is observed with composition-temperature libraries. The combinatorial method is validated by comparison to previous results (12). The results show that high-throughput experimentation is useful not only for the discovery of new materials, but also for observation of fundamental materials properties.

EXPERIMENTAL

To provide neutron scattering contrast, a deuterium labeled model polystyrene (dPS) with a weight average molecular weight $M_w = 102,000$ and polydispersity $M_w/M_n < 1.05$ was used. [According to ISO 3-8, the term "molecular weight" has been replaced with "relative molecular mass," Mr. The conventional notation, rather than the ISO notation, has been employed in the present article.] The PVME was prepared by cationic polymerization as described previously (12), and has an M_w of 119,000 and $M_w/M_n \sim 2.5$. For some of the thin film studies performed using light scattering and AFM measurements, a protonated PS (hPS) sample was used with an $M_w = 90,000$ and $M_w/M_n < 1.05$.

The layered silicates employed in this study belong to the class of 2:1 mica type layered silicates and were suitably organically modified to make compatible with the polymers. Specifically, we have used a dimethyl dioctadecyl ammonium modified montmorillonite (2C18M) as the layered silicates. Montmorillonite is a naturally occurring layered silicate with a lateral disk diameter of approximately 0.5 to 1.0 μm, a thickness of 0.95 nm, and a charge exchange capacity of 90 meq/100 g. These 2C18M layered silicates are intercalated by polystyrene and polyvinylmethylether and are not preferentially attractive to either polymer (4, 13–15).

Small angle neutron scattering (SANS) measurements were performed at the NIST Center for Neutron Research on the 30 m SANS instrument (NG7) and the 8 m SANS instrument (NG1). Neutrons with wavelength 6 Å and a sample to detector distances ranging from 3.6 m to 13 m were used, providing an accessible q-range of 0.003 to 0.1 Å⁻¹. Correction for parasitic background scattering and empty quartz cell scattering were performed using standard protocols described previously (12). The data were also converted to an absolute scale using a secondary standard. Finally, the q-independent background incoherent scattering, primarily because of hydrogen atoms, was removed by scaling the scattering from a pure protonated polymer sample by the proton density in the scattering volume.

Our high-throughput method for studying polymer blend phase separation involves the creation of libraries with orthogonal gradients in blend composition and temperature. Three steps are involved in preparing

composition gradient films: gradient mixing, deposition, and film spreading. Two syringe pumps (Harvard PHD2000), introduce and withdraw polymer solutions to and from a mixing vial at rates I and W, respectively, where I = W = 1.7 ml/min. Pump I contained mass fraction $x_{PS,O} = 0.080$ of PS ($M_w = 96.4$ kg/mol, $M_w/M_n = 1.01$, Tosoh) in toluene. The vial was loaded with an initial Mo = 2.0 ml of mass fraction $x_{PVME,O} = 0.080$ of PVME ($M_w = 119$ kg/mol, $M_w/M_n = 2.5$) in toluene from pump W. The infusion and withdrawal syringe pumps were started simultaneously while vigorously stirring the vial solution, and a third syringe, S, was used to manually extract solution from the vial. The rates I, W, S, the initial volume in the vial, Mo, and the sampling time control the end points and slope of the composition gradient, which has been verified in situ with FTIR spectroscopy. See ref. (18) for an experimental setup of the composition gradient library preparation method.

Because the sample syringe contains a gradient in the PS and PVME composition along the length of the syringe, molecular diffusion will lead to uniform composition over time. However, the timescale for molecular diffusion is many orders of magnitude larger than the sampling time, since the PS and PVME diffusivities are on the order of 10^{-8} cm²/s. Assuming Fickian diffusion, PS and PVME diffuse in opposite directions in the syringe at 9.3×10^{-11} g/s and 1.5×10^{-10} g/s, respectively. At the point of maximum slope in the ϕ_{PS} gradient, ϕ_{PS} and ϕ_{PVME} change by only 0.004% and 0.001% during the 5-min film deposition process.

Next, the gradient solution from the sample syringe is deposited as a thin 31-mm-long stripe on the silicon substrate. The gradient stripe was quickly placed under a stationary knife-edge of equal length. The gradient stripe was spread as a film, orthogonal to the composition gradient direction, for a distance of 40 mm with the flow coating procedure described above. After a few seconds most of the solvent evaporated, leaving behind a thin film with a gradient of polymer composition. The remaining solvent was removed during the annealing step. The film thickness, measured with ellipsometry, varied monotonically from 345 nm to 510 nm between the low and high PS composition ends, because of viscosity variation in the composition gradient solution. We demonstrated previously that the thickness change due to flow induced by the small thickness gradient (≈ 5 nm/mm) is within the standard uncertainty of ± 3 nm (18).

RESULTS AND DISCUSSION

Based on X-ray diffraction, the layered silicate nanocomposites formed with the two homopolymers and blends with different compositions are consistent with those of intercalated materials—the polymer penetrates the interlayer and swells the silicate layers, but does not cause disruption of the silicate tactoids or stacks (4, 13). The polymer expands the interlayer gallery from an initial separation of 1.3 nm to ~ 2.3 nm

and is consistent with previous studies of Vaia and Giannelis (4, 13). In most of the phase behavior studies performed here, only low quantities of layered-silicate are used, typically never exceeding 2 mass %.

The bulk phase behavior of dPS/PVME blends with 1 and 2 mass % 2C18M was determined by small angle neutron scattering (SANS) measurements. The SANS data were analyzed by using either Zimm analysis or rigorous fitting of the data to the incompressible binary and ternary random phase approximation (16). A summary of typical SANS data is shown in *Fig. 1*, where the extrapolated zero angle scattering (I(0)) is plotted as a function of 1/T. Based on that data and extrapolation to 1/I(0) to zero, it is clear that for the case of dPS/PVME mixtures, the addition of up to 2 mass % 2C18M has a negligible effect on the location of the phase boundaries and the detailed thermodynamic interactions, at least near the LCST.

In an effort to determine the effect of added layered silicate on the phase behavior of PS/PVME mixtures, we undertook measurements of thin films of this blend and nanocomposites with layered silicates using optical microscopy (18) and atomic force microscopy (19). The unfilled blend thin film, when heated to the melt state, exhibited dewetting from the silicon substrate. For the case of added 2C18M to the hPS/PVME blend, we found that the addition of even 1 mass % layered-silicate led to significant stabilization of the blend on the silicon substrate, which was consistent with the previous results (11, 20). Further, atomic force microscopy of the phase-separated structure (upon heating the

blends to the two-phase region above the LCST) suggested a change in the mechanism of phase separation upon addition of layered silicate to the blend. Such a change in mechanism of phase separation is in fact consistent with previous theoretical suggestions and experimental observations (20–22). Additionally, using optical microscopy we observe a strong dependence on the size of the layered-silicate on the phase separation behavior of the thin films of PS and PVME (23).

Figure 2 shows a photograph of a typical temperature-composition library after 2 h of annealing, in which the LCST phase boundary can be seen with the unaided eye as a diffuse curve. Cloud points measured with conventional light scattering are shown as discrete data points and agree well with the phase boundary observed on the library. The diffuse nature of the phase boundary reflects the natural dependence of the microstructure evolution rate on temperature and composition. Near the LCST boundary, the microstructure size gradually approaches optical resolution limits (1 mm), giving the curve its diffuse appearance. Further, significant dewetting of the polymer from the silicon surface is also observed. However, the quantitative agreement of the asymmetric shape and values of the LCST boundary with bulk cloud point values validates the library deposition method and high-throughput approach for mapping polymer blend phase behavior presented here.

The effect of addition of 2% by mass relative to polymer mass of an organically modified clay (2C18M) in each of the polymer solutions allowed us to study the
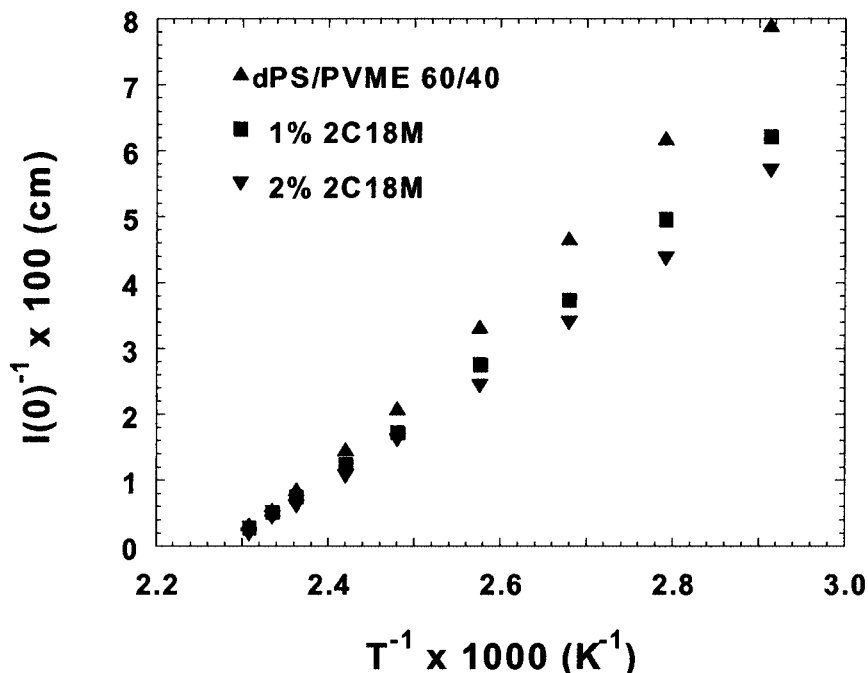

Fig. 1. The extrapolated zero angle coherent neutron scattering intensity (I(0)) for 60/40 mixtures of dPS/PVME and for the two nanocomposites prepared with 1 and 2 mass % dimethyl dioctadecyl ammonium modified montmorillonite (2C18M). The data indicate that the location of the spinodal temperature (obtained by extrapolation of 1/I(0) to zero) is unaffected by the addition of up to 2 mass % 2C18M.

Fig. 2. Photograph of a combinatorial library indicating the known LCST phase boundary for PS-PVME (previously published in ref. 18). For validation, the white points are conventional light scattering cloud points for known compositions of the PS and PVME used in the combinatorial library. (See ref. 18 for experimental setup of composition gradient library method.)
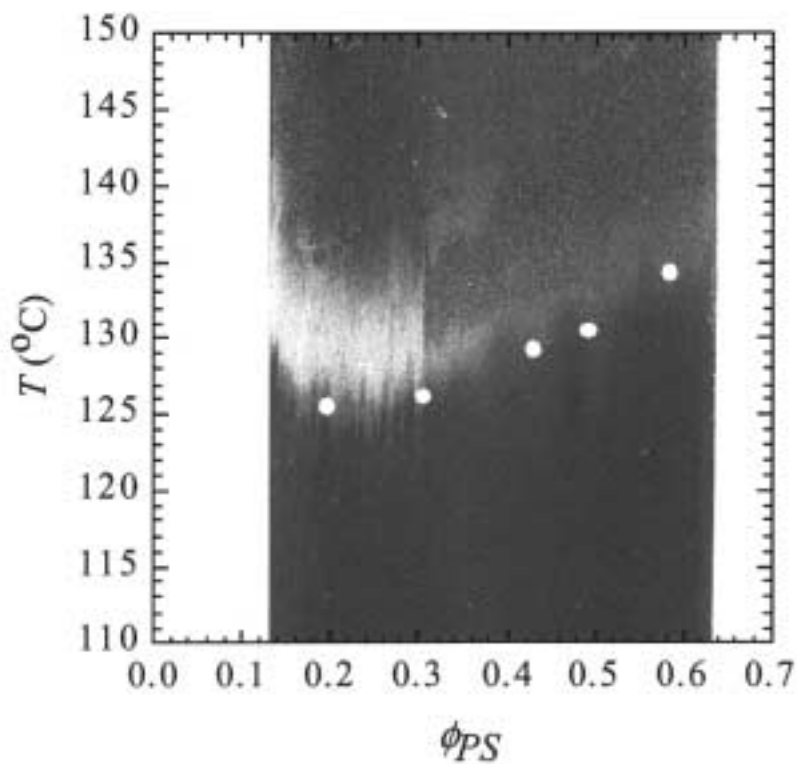

Fig. 3. Photograph of a combinatorial library demonstrating the influence of 2 mass % 2C18M on the phase diagram of dPS and PVME. The dPS/PVME phase diagram is similar to the PS/PVME phase diagram shown in Fig. 2, except for a shift of the phase boundary to higher temperatures because of the influence of isotopic substitution. This figure shows that the effect of the added organically modified has minimal effect on the phase boundary. However, the morphology of structures determined at higher magnification inside the phase-separated region are modified by the clay.
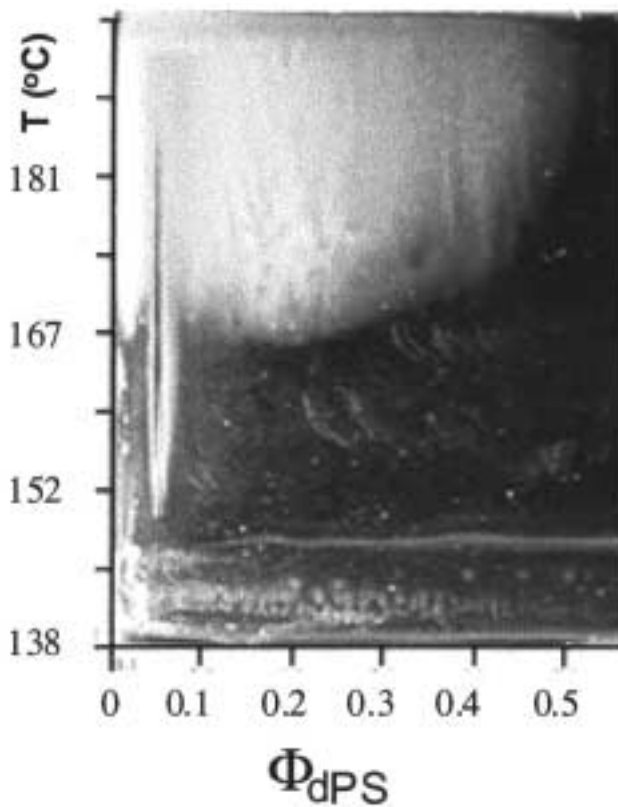
effect of layered silicates on the phase behavior and morphology of the dPS/PVME system. *Figure 3* demonstrates the combinatorial phase boundary of this layered silicate (2C18M)/dPS/PVME system. While the phase boundary of this deuterated polymer system is not significantly affected by the addition of the clay, the evolution of morphology of the phase-separated structures (as imaged at much higher magnification by optical and atomic force microscopy) inside the phase boundary is different. A more detailed study is under way to characterize this difference in morphology with the addition of the clay.

CONCLUSIONS

Based on detailed small angle neutron scattering measurements, we deduce that the location of the spinodal temperature is essentially unaffected by the addition of up to 2 mass % organically modified layered silicate. Optical microscopy in conjunction with high throughput combinatorial methods corroborates these inferences by a direct mapping of the phase diagram. The effect of an organically modified layered silicate on the cloud point phase boundary was found to be minimal. However, there are changes to the morphological structure with the addition of the clay.

ACKNOWLEDGMENTS

REFERENCES

1. E. P. Giannelis, R. Krishnamoorti, and E. Manias, *Adv. Polym. Sci.*, **138**, 107–147 (1999).
2. A. Usuki, Y. Kojima, M. Kawasumi, A. Okada, Y. Fukushima, T. Kurauchi, and O. Kamigaito, *J. Mat. Res.*, **8**, 1174 (1993).
3. A. Usuki, A. Koiwai, Y. Kojima, M. Kawasumi, A. Okada, T. Kurauchi, and O. Kamigaito, *J. Appl. Polym. Sci.*, **55**, 119 (1995).
4. R. A. Vaia and E. P. Giannelis, *Macromolecules*, **30**, 7990 (1997).
5. P. B. Messersmith and E. P. Giannelis, *Chem. Mater.*, **5**, 1064 (1993).
6. P. B. Messersmith and E. P. Giannelis, *Chem. Mater.*, **6**, 1719 (1994).
7. P. B. Messersmith and E. P. Giannelis, *J. Polym. Sci.: Part A: Polym. Chem.*, **33**, 1047 (1995).
8. G. H. Fredrickson and J. Bicerano, *J. Chemical Physics*, **110**, 2181 (1999).
9. R. Limary and P. F. Green, *Macromolecules*, **32**, 8172 (1999).
10. R. Limary and P. F. Green, *Langmuir*, **15**, 5617 (1999).
11. R. Limary, S. Swinnea, and P. F. Green, *Macromolecules*, **33**, 5227 (2000).
12. C. C. Han, B. J. Bauer, J. C. Clark, Y. Muroga, Y. Matsushita, M. Okada, Q. T. Cong, T. Chang, and I. C. Sanchez, *Polymer*, **29**, 2002 (1988).
13. R. A. Vaia and E. P. Giannelis, *Macromolecules*, **30**, 8000 (1997).
14. R. Krishnamoorti, A. S. Silva, and C. A. Mitchell, *J. Chem. Phys.*, 2001, in press.
15. C. A. Mitchell and R. Krishnamoorti, in *Polymer Nanocomposites*, R. Krishnamoorti and R. A. Vaia, Eds., ACS (2001).
16. P. G. de Gennes, *Scaling Concepts in Polymer Physics*, Cornell University Press, Ithaca, N.Y. (1979).
17. J. J. Hanak, *J. Mat. Sci.*, **5**, 964 (1970); B. Jandeleit, D. J. Schaefer, T. S. Powers, H. W. Turner, and W. H. Weinberg, *Angew. Chem. Int. Ed.*, **38**, 2494 (1999); E. Danielson, M. Devenney, D. M. Giaquinta, J. H. Golden, R. C. Haushalter, E. W. McFarland, D. M. Poojary, C. M. Reaves, W. H. Wenberg, and X. D. Wu, *Science*, **279**, 837 (1998); J. Wang, Y. Yoo, C. Gao, I. Takeuchi, X. Sun, H. Chang, X.-D. Xiang, and P. G. Schultz, *Science*, **279**, 1712 (1998); E. Reddington, A. Sapienza, B. Gurau, R. Viswanathan, S. Sarangapani, E. Smotkin, and T. Mallouk, *Science*, **280**, 1735 (1998); J. Klein, C. W. Lehmann, H.-W. Schmidt, and W. F. Maier, *Angew. Chem. Int. Ed.*, **37**, 3369 (1998); T. Bein, *Angew. Chem. Int. Ed.*, **38**, 323 (1999); T. A. Dickinson, D. R. Walt, J. White, and J. S. Kauer, *Anal. Chem.*, **69**, 3413 (1997); S. Brocchini, K. James, V. Tangpasuthadol, and J. Kohn, *J. Biomed. Mater. Res.*, **42**, 66 (1998).
18. C. J. Meredith, A. Karim, and E. J. Amis, *Macromolecules*, **33**, 5760 (2000).
19. D. Raghavan, X. Gu, T. Nguyen, M. VanLandingham, and A. Karim, *Macromolecules*, **33**, 2573 (2000).
20. K. A. Barnes, A. Karim, J. F. Douglas, A. I. Nakatani, H. Gruell, and E. J. Amis, *Macromolecules*, **33**, 4177 (2000).
21. V. V. Ginzburg, G. Peng, F. Qiu, D. Jasnow, and A. C. Balazs, *Physical Review E*, **60**, 4352 (1999).
22. V. V. Ginzburg, F. Qiu, M. Paniconi, G. Peng, D. Jasnow, and A. C. Balazs, *Physical Review Letters*, **82**, 4026 (1999).
23. K. Yurekli, R. Krishnamoorti, and A. Karim, in preparation.